

# ELECTROMAGNETIC DESIGN OF 400 MHz RF-DIPOLE CRABBING CAVITY FOR LHC HIGH LUMINOSITY UPGRADE\*

S. U. De Silva<sup>#</sup>, H. Park, J. R. Delayen, Old Dominion University, Norfolk, VA, USA  
Z. Li, SLAC National Accelerator Laboratory, Menlo Park, CA USA

## Abstract

The beam crabbing proposed for the LHC High Luminosity Upgrade requires two crabbing systems operating in both horizontal and vertical planes. In addition, the crabbing cavity design needs to meet strict dimensional constraints and functional specifications of the cavities. This paper presents the detailed electromagnetic design including rf properties, multipole analysis, multipacting levels of the 400 MHz rf-dipole crabbing cavity.

## INTRODUCTION

The LHC High Luminosity Upgrade is proposed to use crabbing cavities for its 14 TeV beam operation. The crabbing cavities are expected to increase the luminosity at the interaction point (IP) provide luminosity levelling to reduce pile up at IP. The parallel beam pipes in the LHC sets strict dimensional constraints on the crabbing cavity system, hence requires compact crabbing cavities [1]. The rf-dipole cavity is one of the two 400 MHz crabbing cavities and will be used for horizontal crabbing of the proton beams at LHC. Prior to installation at LHC the proposed cavities will be tested at Point-6 in SPS at CERN.

## RF-DIPOLE CRABBING CAVITY

A cylindrical shaped proof-of-principle (P-o-P) cavity has been designed, fabricated and successfully tested [2, 3]. The P-o-P cavity achieved at transverse voltage of 7.0 MV with an intrinsic quality factor of  $1.25 \times 10^{10}$  [2, 3].

The 400 MHz crabbing cavity for LHC high luminosity upgrade is adapted into a square shaped design to meet the dimensional constraints. The compact crabbing cavity is optimized to meet the current requirements for LHC [4].

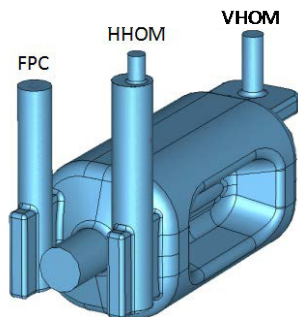


Figure 1: 400 MHz rf-dipole prototype cavity for LHC high-luminosity upgrade.

The 400 MHz rf-dipole cavity shown in Fig. 1 operates in a  $TE_{11}$  like mode where the contribution to the transverse voltage is primarily due to the transverse electric field. The cavity is designed with transverse dimensions less than 285 mm, in order to accommodate the parallel beam line in the LHC. Hence the prototype cavity is designed with a square shaped outer conductor where all the ancillary components of the cavity are designed on the end plate of the cavity as shown in Fig. 1. Table 1 shows the cavity parameters and rf properties of the prototype cavity.

Table 1: RF Properties of Prototype RF-dipole Cavity

Parameter	Value	Units
Cavity length	775	mm
Cavity diameter	281	mm
Aperture diameter	84	mm
Deflecting voltage ( $V_T^*$ )	0.375	MV
Peak electric field ( $E_P^*$ )	3.6	MV/m
Peak magnetic field ( $B_P^*$ )	6.2	mT
$B_P^* / E_P^*$	1.71	mT/(MV/m)
Energy content ( $U^*$ )	0.13	J
Geometrical factor	107	$\Omega$
$[R/Q]_T$	430	$\Omega$
$R_T R_S$	$4.6 \times 10^4$	$\Omega^2$

At  $E_T^* = 1$  MV/m

Table 2 shows the operational parameters expected to be achieved at 3.4 MV and with the projected parameters of operation at 5.0 MV for the rf-dipole cavity. The cavities will be operated at 2.0 K and the power dissipation is determined assuming a surface resistance of  $R_s = 11.3$  n $\Omega$  with a residual surface resistance of  $R_{res} = 10$  n $\Omega$ .

Table 2: Operating Parameters at 3.4 MV and 5.0 MV

Parameter	(A)	(B)	Units
Deflecting voltage ( $V_T$ )	3.4	5.0	MV
Intrinsic quality factor ( $Q_0$ )	9.5		$\times 10^9$
Peak electric field ( $E_P$ )	34	50	MV/m
Peak magnetic field ( $B_P$ )	57	84	mT
Power dissipation ( $P_{diss}$ )	2.8	6.2	W

The ancillary component of the rf-dipole crabbing cavity is designed to meet the current specifications for the SPS beam test at CERN [1]. The fundamental power coupler is designed to achieve a coupling of  $5.5 \times 10^5$  [5]. The optimized coupler hook has a reduced power

\*Work supported by DOE via US LARP Program and by the High Luminosity LHC Project. Work was also supported by DOE Contract No. DE-AC02-76SF00515.

<sup>#</sup>sdesilva@jlab.org

dissipation of 69 W. The fundamental power coupler is under fabrication at CERN [6].

### HIGHER ORDER MODE DAMPING

The higher order mode (HOM) spectrum for the rf-dipole cavity up to 2 GHz is shown in Fig. 2. One of the attractive features of the rf-dipole geometry is that there are no lower modes, and the frequency of the nearest HOM is 1.5 times the fundamental mode.

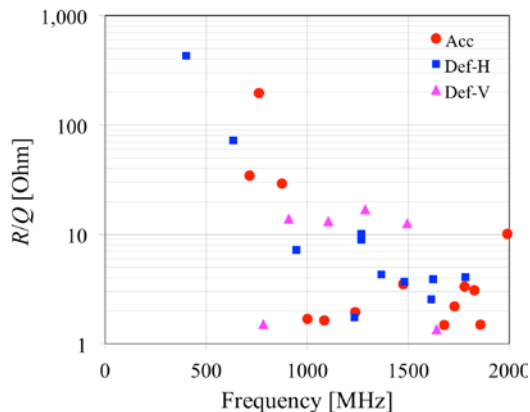


Figure 2: [R/Q] values of the rf-dipole cavity.

#### Higher Order Mode Couplers

The current impedance specifications [7] for damping of HOMs are achieved with two HOM couplers as shown in Fig. 3. The horizontal HOM (HHOM) coupler damps the higher order horizontal deflecting modes and some of the accelerating modes, and the vertical HOM (VHOM) coupler damps the vertical deflecting modes. Accelerating modes present in the cavity are damped by both HHOM and VHOM.

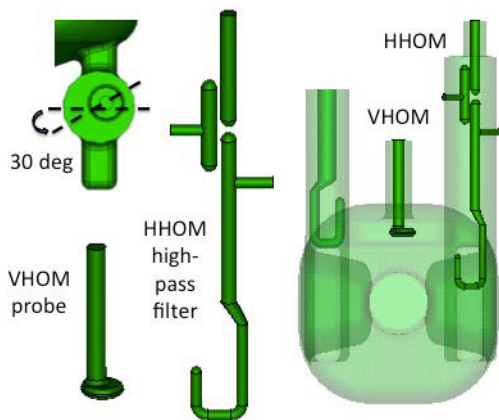


Figure 3: HOM couplers for the rf-dipole cavity: horizontal and vertical (HHOM & VHOM) couplers.

The HOM coupler designs have been improved by Z. Li to effectively damp some of the transverse modes at higher frequencies with higher impedance [5]. The HHOM coupler is rotated 30° deg as shown in Fig. 3 and the modified hook in the high pass filter strongly damps the two HOMs above 1900 MHz with high transverse impedance to ~1.0 MΩ/m. The VHOM probe has been modified as shown in Fig. 3 to suppress vertical

deflecting modes. The corresponding  $Q_{ext}$  with longitudinal and transverse impedance ( $Z_z$  and  $Z_T$ ) values are shown in Fig. 4.

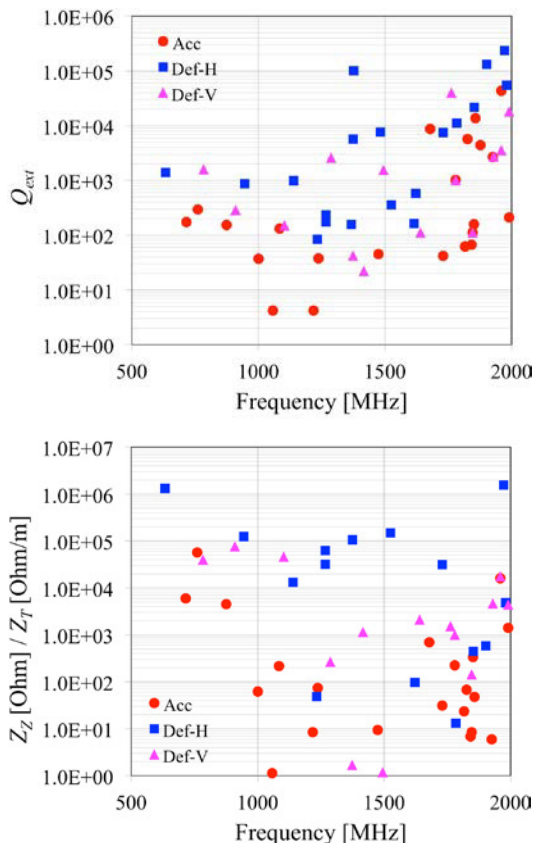


Figure 4:  $Q_{ext}$  and corresponding longitudinal and transverse impedance ( $Z_z$  and  $Z_T$ ) of the HOMs of the rf-dipole cavity.

#### Mechanical Tolerances

The fabrication, assembly, and processing of the cavity and HOM couplers during the manufacturing process may introduce deviations from the ideal shape. These deviations may reduce the effectiveness in HOM damping increasing the impedance. Additionally, the deviations may also contribute to the power dissipation due to the fundamental mode. Therefore, a complete scan of cavity and HOM coupler deviations are studied to determine the tolerances on the HHOM coupler to determine the acceptable levels of deviations and tolerances required to be achieved during machining and processing [8].

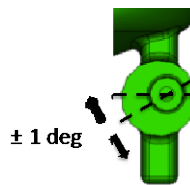


Figure 5: Rotational deviations of HHOM hook.

The dependence on the HOM damping due to rotational and translational deviations of the cavity and HHOM coupler are presented in Ref. [8]. In addition, the

rotational deviation of the HHOM hook along the vertical axis (y axis) as shown in Fig. 5 are analysed for the improved HHOM coupler.

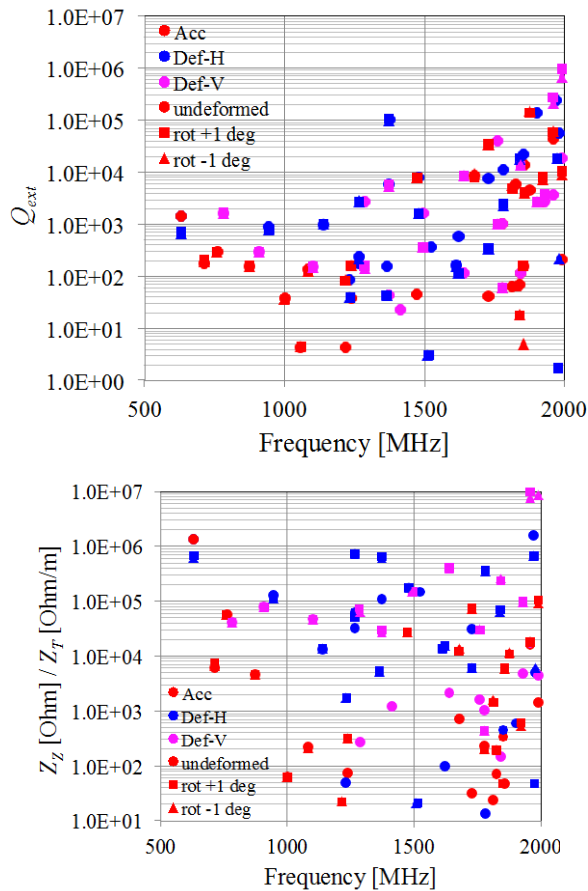


Figure 6:  $Q_{ext}$  (top), and  $Z_z$  and  $Z_T$  (bottom) for rotational deviations of  $\pm 1.0$  deg of the HHOM hook.

The  $Q_{ext}$  and impedance of the HOMs for deviations of  $\pm 1.0$  deg in comparison to the undeformed cavity are shown in Fig. 6. The HOM damping is sensitive to the rotational deviations of the hook. Therefore, any deviations of the HOM hook is required to keep at a minimum and well controlled to maintain the HOM damping at the design level.

### Thermal Analysis

The rf heating caused by the beam induced voltage in the HOM couplers in the crabbing cavity system is required to be extracted by conduction or convection cooling. The HOM heating is determined assuming a 1 kW of HOM power propagating through the HOM couplers. The HHOM coupler consists of the hook and T made of Nb, and Cu probe and gasket. The rf heating determined for the fundamental mode at the hook is 0.733 mW, less than 0.1 W at the probe and less than 1 mW on the Cu gasket. A surface resistance of 10 nΩ is assumed for the Nb parts, and for the Cu probe and gasket the surface resistance was scaled following the anomalous limit for a normal conductor at the room temperature. Therefore, the assumed surface resistance at 400 MHz is

5 mΩ. The loss at the RF copper gasket is calculated assuming a surface resistance of 1 mΩ at 2K.

The heat load applied on the HHOM coupler includes the heating due to the fundamental mode and a HOM with the highest losses [9]. The finite element analysis shows the temperature increase about 0.1 K at the niobium hook extremity, 0.24 K at the copper gasket. The temperature profile was checked against the initial assumption of the temperature dependent surface resistance. The results assure the temperature is converging to a stable point.

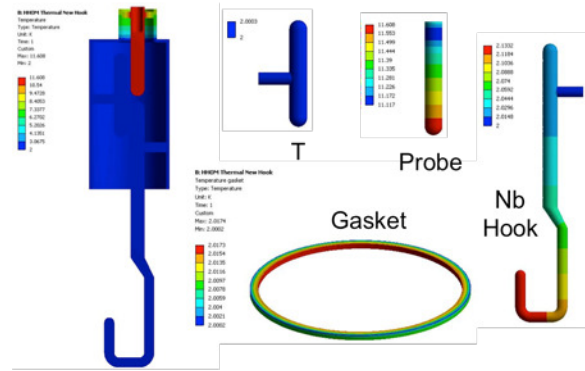


Figure 7: Temperature profile [unit in K].

Figure 7 shows the temperature profile of each component in the HHOM coupler calculated with Ansys. The total temperature increases in the hook is less than 0.15 K and 0.017 K on the gasket. The increase in temperature at the T is negligible. The probe temperature increase is about 0.5 K. The temperature increases are well within the design limitations.

### Multipole Analysis

The rf-dipole cavity is designed with curved loading elements as shown in Fig. 8, where the higher order multipole components are shown in Table 3. The even order components are zero for the rf-dipole geometry. The primary requirement is to minimize the  $b_3$  component below  $10^3$  mT/m<sup>2</sup>.

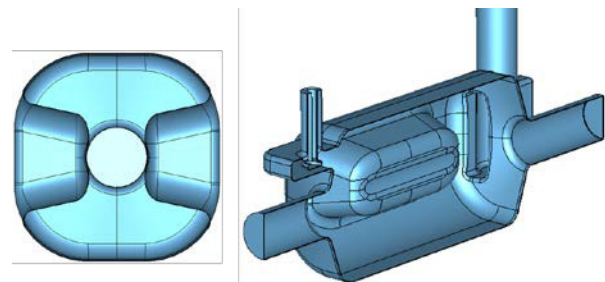


Figure 8: RF-dipole cavity with curved loading elements.

Table 3: Higher Order Multipole Components at 1.0 MV

Component	Bare Cavity	Full Cavity	Units
$b_1$	3.3	3.3	mT/m
$b_3$	39	47	mT/m <sup>2</sup>
$b_5$	$2.0 \times 10^5$	$2.0 \times 10^5$	mT/m <sup>4</sup>

*Multipacting Analysis*

The multipacting levels for the crabbing cavity were analysed using the Track3P of SLAC ACE3P suite [10]. The prototype cavity body has low multipacting levels compared to the P-o-P cavity [2]. The resonant particle location on the cavity is shown in Fig. 9 where Fig. 10 shows the impact energy of the resonant particles with varying transverse voltage. The resonant particles are primarily located end plates, around poles and at the fundamental power coupler. There are no multipacting levels at the HOM couplers. The multipacting levels expected to be processed easily similar to the P-o-P cavity.

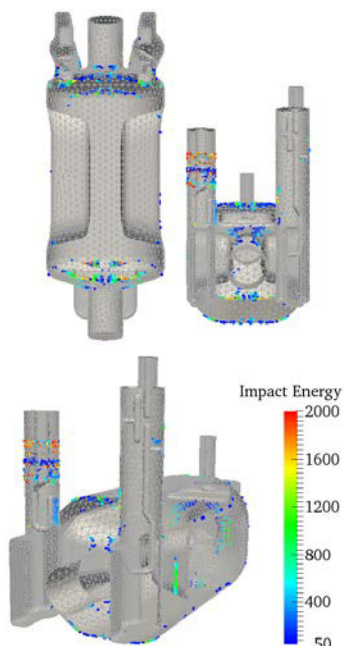


Figure 9: Resonant particles on the rf-dipole cavity.

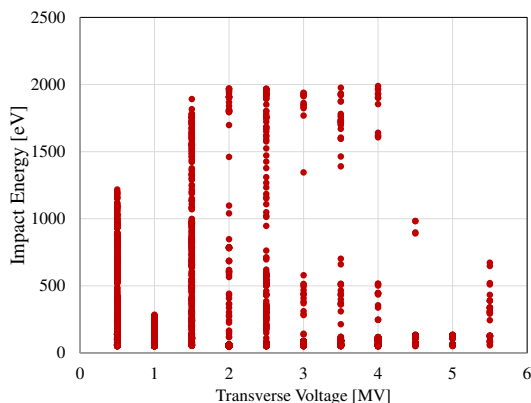


Figure 10: Impact energy of the resonant particles as a function of transverse voltage.

**HELIUM VESSEL AND CRYOMODULE**

The SPS cryomodule consists of two crabbing cavities. The cryomodule design with dressed cavities including tuners and all the ancillary components are on going.

Figure 11 shows the rf-dipole cavity with interfaces, magnetic shielding and helium vessel [11-14].

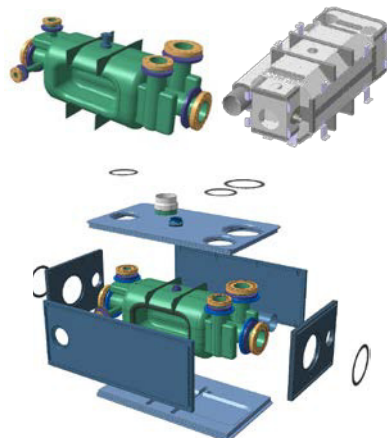


Figure 11: Cavity with interfaces (top left), magnetic shielding (top right) and helium vessel (bottom) for the rf-dipole cavity.

**RF-DIPOLE CAVITY WITH 100 mm BEAM APERTURE**

The impedance study for the LHC may require achieving lower transverse impedances for the HOMs of the crabbing cavities. The current design may be limited in achieving further damping of the higher order modes. Therefore, a revised crabbing cavity design with a 100 mm beam aperture is being considered. Figure 12 shows the two rf-dipole cavities with beam apertures of 84 mm and 100 mm.

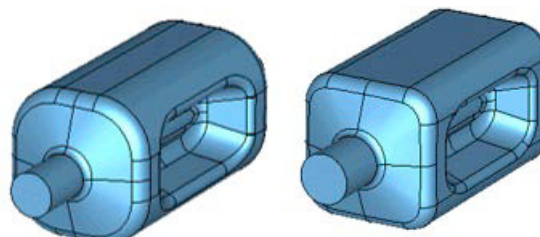


Figure 12: RF-dipole cavities with beam apertures of 84 mm and 100 mm.

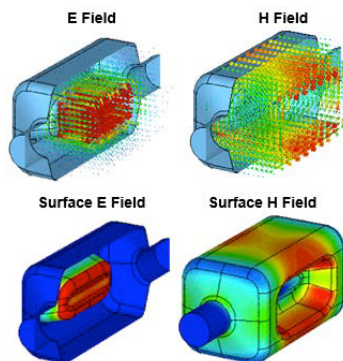


Figure 13: Electric and magnetic fields (top) and surface electric and magnetic fields (bottom) of the rf-dipole cavity 100 mm beam aperture.

Figure 13 shows the electromagnetic field profile of the cavity. Table 4 gives the rf properties of revised design. The peak surface fields increases by 10–15 % with reduction in the shunt impedance by 30%. Therefore, the cavity will operate at slightly higher peak fields of 40 MV/m and 64 mT at the nominal transverse voltage of 3.4 MV. Further analysis of multipole components and HOM damping is underway.

Table 4: RF Properties of RF-dipole Cavities with (A) 84 mm and (B) 100 mm Beam Aperture Diameters.

Parameter	(A)	(B)	Units
Frequency	400		MHz
Aperture diameter	84	100	mm
Nearest HOM	633.5	630.0	mm
Peak electric field ( $E_p^*$ )	3.6	4.2	MV/m
Peak magnetic field ( $B_p^*$ )	6.2	6.9	mT
$B_p^* / E_p^*$	1.71	1.66	mT/ (MV/m)
Geometrical factor	107	112	$\Omega$
$[R/Q]_T$	430	278	$\Omega$
$R_T R_S$	$4.6 \times 10^4$	$3.1 \times 10^4$	$\Omega^2$

At  $E_T^* = 1$  MV/m

## CONCLUSION

The 400 MHz rf-dipole crabbing cavity design is completed to meet the dimensional constraints and rf requirements of the crabbing cavities for the LHC high luminosity upgrade. The SPS cryomodule design consisting of two dressed cavities will be adapted for the LHC operation. The on-going impedance analysis of LHC may lead to tighter impedance requirements that will limit the existing cavity performance. The rf-dipole cavity design with 100 mm beam aperture is an alternate option in achieving improved HOM damping without increasing the number of cavities of the existing design, operating at a lower transverse kick. The modified designs can be easily adapted to meet the other design requirements.

## ACKNOWLEDGEMENTS

We would like to thank R. Calaga, O. Capatina, C. Zanoni, K. Artoos, F. Carra, and T. Capelli at CERN for the engineering design. We also would like to thank G. Burt, A. Tutte, T. Jones and N. Templton at Lancaster University and STFC, UK and Alessandro Ratti at LBNL.

This research used resources of the National Energy Research Scientific Computing Center, which is supported by the Office of Science of the U. S. Department of Energy under Contract No. DE-AC02-05CH11231.

## REFERENCES

- [1] P. Baudreghien et al., Functional Specifications of the LHC Prototype Crab Cavity System, Tech. Rep. CERN-ACC-NOTE-2013-003 (CERN, 2013).
- [2] S. U. De Silva and J. R. Delayen, Phys. Rev. ST Accel. Beams **16**, 082001 (2013).
- [3] S. U. De Silva et al., “Design and Prototyping of a 400 MHz RF-Dipole Crabbing Cavity for the LHC High-Luminosity Upgrade”, Proceedings of IPAC 2015, Richmond, VA, USA (2015), p. 3568.
- [4] S. U. De Silva, Ph.D. Thesis, Old Dominion University, 2014.
- [5] Z. Li et al., “FPC and Hi-Pass Filter HOM Coupler Design for the RF Dipole Crab Cavity for the LHC HiLumi Upgrade”, Proceedings of IPAC 2015, Richmond, VA, USA (2015), p. 3492.
- [6] E. Montesinos, “RF Power and Coupler Status”, HiLumi-LHC/LARP Crab Cavity System External Review, BNL, May 2014.
- [7] N. Biancacci, “HL-LHC Impedance and Stability Studies”, Joint HiLumi-LARP Meeting and 24<sup>th</sup> LARP Collaboration Meeting, FNAL, May 2015.
- [8] S. U. De Silva et al., “Imperfection and Tolerance Analysis of HOM Couplers for LHC High-Luminosity Upgrade”, Proceedings of IPAC 2015, Richmond, VA, USA (2015), p. 3572.
- [9] H. Park et al., “Engineering Study of Crab Cavity HOM Couplers for LHC High Luminosity Upgrade”, Proceedings of IPAC 2015, Richmond, VA, USA (2015), p. 3578.
- [10] K. Ko et al., “Advances in Parallel Electromagnetic Codes for Accelerator Science and Development,” FR101, Proc. LINAC2010, Tsukuba, Japan (2010).
- [11] C. Zanoni et al., “Design of Dressed Crab Cavities for the High Luminosity LHC Upgrade”, *these proceedings*, THPB070, Proc. SRF2015, Whistler, Canada (2015).
- [12] K. Artoos et al., “Development of SRF Cavity Tuners for CERN”, *these proceedings*, THPB060, Proc. SRF2015, Whistler, Canada (2015).
- [13] N. Templton et al., “Design of the Thermal and Magnetic Shielding”, *these proceedings*, TUPB101, Proc. SRF2015, Whistler, Canada (2015).
- [14] F. Carra et al., “Crab Cavity and Cryomodule Development for HL-LHC”, *these proceedings*, FRBA02, Proc. SRF2015, Whistler, Canada (2015).